

Article

A Novel Mathematical Model Considering Real Gas PVT Behavior to Estimate Inflow Performance Relationship of Gas Well Production

Shuang Zhang , Huiqing Liu *, Yanwei Wang, Ke Sun and Yunfei Guo

State Key Laboratory of Petroleum Resources and Prospecting, China University of Petroleum, Beijing 102249, China; 2015312056@student.cup.edu.cn (S.Z.); 2017312036@student.cup.edu.cn (Y.W.); 2019310163@student.cup.edu.cn (K.S.); 2019310162@student.cup.edu.cn (Y.G.)

* Correspondence: liuhq@cup.edu.cn

Abstract: Inflow performance relationship (IPR) is one of the most important methods for the analysis of the dynamic characteristics of gas reservoir production. The objective of this study was to develop a model to improve the accuracy of the IPR for evaluating and predicting the production of gas reservoirs. In this paper, a novel mathematical model, taking into account the real gas PVT behavior, is developed to accurately estimate the inflow performance relationship. By introducing a pseudo-pressure function and a real gas properties database, this model eliminates the error caused by the linearization method and improves the calculation accuracy. The results show that more than 90% of the energy in the flow field is consumed by inertial forces, which leads to significant high-velocity non-Darcy effects in the gas reservoir. The reservoir permeability, original reservoir pressure, stress sensitivity coefficient, and skin factor have a great impact on the inflow performance relationship of gas reservoir production. This model predicts gas IPR curves with excellent accuracy and high efficiency. The high-precision gas well inflow performance relationship lays a solid foundation for dynamic production analysis, rational proration, and intelligent development of the gas field.

Keywords: high-velocity non-Darcy flow; inflow performance relationship; real gas PVT behavior; non-linearization; stress sensitive



Citation: Zhang, S.; Liu, H.; Wang, Y.; Sun, K.; Guo, Y. A Novel Mathematical Model Considering Real Gas PVT Behavior to Estimate Inflow Performance Relationship of Gas Well Production. *Energies* **2021**, *14*, 3594. <https://doi.org/10.3390/en14123594>

Academic Editor: Reza Rezaee

Received: 16 May 2021

Accepted: 14 June 2021

Published: 16 June 2021

Publisher's Note: MDPI stays neutral with regard to jurisdictional claims in published maps and institutional affiliations.



Copyright: © 2021 by the authors. Licensee MDPI, Basel, Switzerland. This article is an open access article distributed under the terms and conditions of the Creative Commons Attribution (CC BY) license (<https://creativecommons.org/licenses/by/4.0/>).

1. Introduction

Gas well productivity plays a critical role in gas reservoir engineering. The inflow performance relationship (IPR) of a well is the relationship between its production rate and the flowing bottom hole pressure. The evaluation and prediction of the inflow performance of gas wells are vital steps in developing new gas fields, optimizing the production performance of existing wells, and designing new wells.

Based on previous studies on oil flow in porous media, numerous gas flow models were developed from those of oil flow [1–8]. For oil wells, the fluid flow rate is usually assumed to be proportional to the difference between reservoir pressure and well bottom hole pressure [9], and this assumption leads to a linear relationship for the steady-state flow of incompressible single-phase fluid. Many scholars have studied many factors to improve the IPR accuracy of oil wells. Dietz [10] proposed a variety of shape factors to describe the asymmetrical positioning of a well. Economides [11] presented two correlations for the skin effect in steady- and pseudo-state in a circular drainage area. However, there are notable differences between gas flow and liquid flow in terms of physical characteristics. For example, gas density varies with pressure, while crude oil density is usually treated as a constant. These significant differences have caused some simplifications for oil flow to be ineffective in gas flow.

To accurately characterize the influence of real gas properties on gas flow, many scholars have proposed their linearization methods as follows: (1) Pressure square method [11–14]

—for pressures less than 2000 psi, the product of the compressibility factor Z and viscosity μ is a constant. The real gas pseudo-pressure $m(p)$ shows a linear relationship with the square of pressure. (2) Pressure approximation method [15–19]—when the bottom hole flowing pressure is higher than 3000 psi, the product of the compressibility factor Z and viscosity μ is roughly proportional to the pressure. The real gas pseudo-pressure $m(p)$ shows a linear relationship with pressure. (3) Pseudo-pressure method [20–23]—this method can be applied in a wide range of pressures without any error. Al-Hussainy et al. [24] defined the pseudo-pressure to derive a quadratic gas deliverability equation for the boundary-dominated flow period. Raghavan et al. [25] defined the pseudo-pressure to obtain solutions to nonlinear flow equations in which reservoir and fluid properties are pressure dependent. Samaniego et al. [26] studied the application of the $m(p)$ method to drawdown, buildup, injection, and falloff testing. Samaniego et al. [27] presented a performance-prediction procedure based on the drainage radius concept and a material-balance equation.

The pressure square method and the pressure approximation method can only be applied under their constraints. According to the limited gas well test data, the gas flow equation is linearized to obtain the analytical gas well IPR whose coefficients are strongly dependent on pressure. It is unreasonable to use the absolute open flow rate extrapolated by IPR to guide the gas reservoir production. The linearization method reduces the degree of nonlinearity of the gas flow equation, which is convenient for solving nonlinear equations analytically. However, the linearization method is an approximate method, which will produce inevitable errors in the process.

The accuracy of the real gas PVT behavior is critical to all analytical and numerical gas flow models. Some empirical formulas, algorithms, and software are introduced to describe the real-gas PVT behavior accurately. Dranchuk et al. [28] used the BWR equation of state to fit the compressibility factor of the natural gas. Lee et al. [29] used eight samples to fit the viscosity of natural gas at high pressure. However, these empirical formulas fitted from limited test data cannot cover all situations, and the errors in the fitting process cannot be eliminated. The model presented in this paper uses the Reference Fluid Thermodynamic and Transport Properties (REFPROP) database as real gas properties data. The REFPROP database program is widely used in the refrigeration industry for the calculation of refrigerant properties. REFPROP is an international authoritative working substance physical property calculation software developed by the National Institute of Standards and Technology (NIST) (Version 9.0, Boulder, CO, USA) [30]. Judging from the previous studies, REFPROP is used by many research projects as a physical data source or as a reference data source for the accuracy of calculation results [31].

Furthermore, several specific factors different from those in oil flow should be considered for gas flow in porous media. The high-velocity non-Darcy effect characterized by Forchheimer's equation has a great influence on the gas flow. In 1901, Forchheimer [32] found that Darcy's law was inadequate to describe high-velocity gas flow in porous media and added an additional pressure drop predicted by Darcy's law in order to account for the discrepancy. Aronofsky and Jenkins [12] developed the solution for a vertical well at steady state from the solution of the differential equation for gas flow through porous media by using the non-Darcy factor. Smith [33] and Swift and Kiel [34] indicated that a non-Darcy flow of gases leads to an additional pressure drop near the wellbore, which can be treated as a rate-dependent skin factor. Jones [13] proposed a correlation that includes the Forchheimer factor β . Odeh [14] derived the pseudo-steady-state flow equation with a noncircular drainage area. Economides [11] suggested a steady-state flow equation for horizontal wells. However, the Forchheimer factor β and turbulence coefficient D calculated at the well bottom condition are used as constants to describe the degree of the non-Darcy effect. The influence of the non-Darcy effect on the entire flow field is not considered. Moreover, the impact of stress sensitivity on the inflow performance should be regarded as in the fractured gas reservoir. Yang et al. [35], Li et al. [36], and Zhang et al. [37] took the features of high-speed non-Darcy flow into consideration but neglected the characteristics

of media formation. Clarkson et al. [38] investigated the impact of both stress-dependent matrix permeability and fracture-conductivity changes on rate-transient signatures and derived reservoir and hydraulic-fracture properties.

In this paper, taking into account the real gas PVT behavior, a novel high-velocity non-Darcy flow model is proposed by introducing a pseudo-pressure function with high nonlinearity to accurately estimate the inflow performance relationship of gas reservoir production. Then, the REFPROP database is introduced as a physical property data source to determine the real gas PVT behavior that can adapt to a wide range of reservoir conditions, which greatly improves the accuracy of the physical property parameters of the model. On this basis, the proposed model is verified by field data, and compared with the traditional model using linear approximate solution. Finally, the effects of reservoir permeability, original reservoir pressure, initial gas saturation, stress sensitivity coefficient, and skin factor on the inflow performance relationship of gas reservoir production are analyzed by this model. This research highlights the enormous potential of replacing traditional linear models and predicting the inflow performance relationship with higher accuracy in the field.

2. Model Description

A gas well is the basic unit of gas reservoir development, and accurate evaluation of gas well productivity is the key to efficient and reasonable development of gas reservoirs. The conceptual illustration of a vertical gas-producing well in a carbonate reservoir is shown in Figure 1.

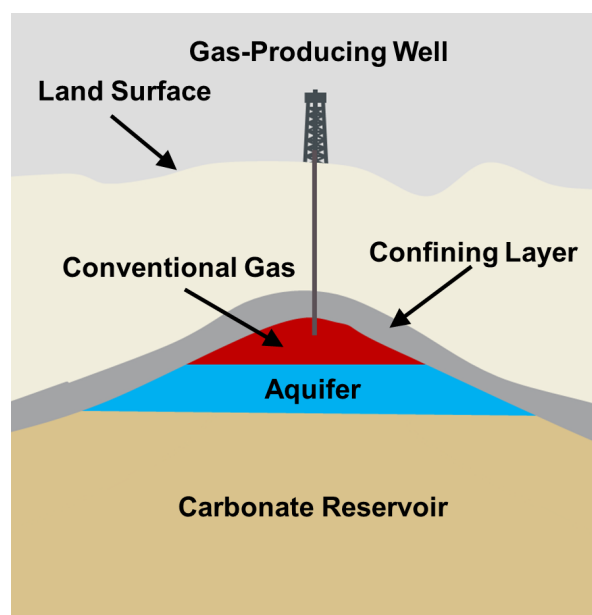


Figure 1. Schematic diagram of a vertical gas-producing well in a carbonate reservoir.

2.1. General Assumptions

In order to study the gas well inflow performance relationship, a schematic diagram of gas reservoir model is shown in Figure 2, and some basic assumptions are made as follows:

1. The reservoir is disk shaped, with its center at the wellbore, and it is a homogeneous and isotropic formation with uniform thickness. The upper and lower boundaries of the reservoir are closed, and the supply boundary pressure is constant at P_e .
2. The formation has the same permeability and porosity. Both properties are stress-sensitive.
3. The only flowing phase is gas phase with unsteady state.
4. The well completion method is open hole completion.
5. Gravitational forces are negligible.

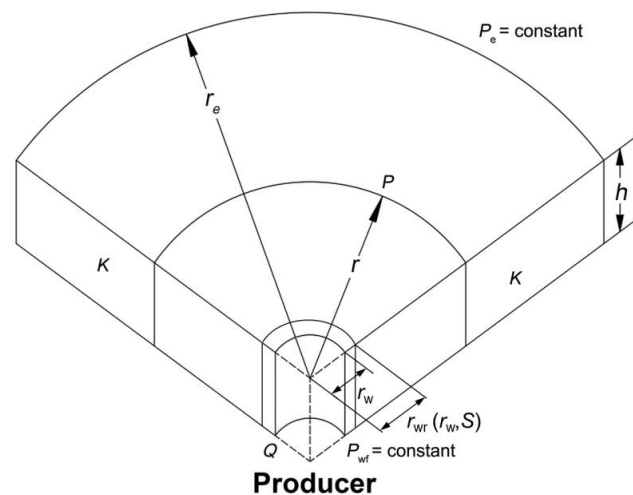


Figure 2. Schematic diagram of the gas reservoir model.

2.2. Mathematical Model of Radial Flow in Gas Reservoir

To study the non-Darcy flow effect, the equation proposed by Forchheimer [32] is used in this model. The flow law equation in SI units is given as follows:

$$-\frac{\partial P}{\partial r} = \frac{\mu_g}{K} v_g + \beta \rho_g v_g^2 \quad (1)$$

where ρ is the gas density, μ is the gas viscosity, K is the permeability, and v_g is the gas velocity. At high flow rate, the gas flow is dominated by the inertial forces, and the magnitude of the viscous force is constant. In the laminar flow situation, there is no inertial force item in Equation (1).

Equation (1) can be rewritten as:

$$-\frac{\partial P}{\partial r} = a v_g + b v_g^2 \quad (2)$$

where

$$a = \frac{\mu_g}{K} \quad (3)$$

$$b = \beta \rho_g \quad (4)$$

The parameter β is given by three relations, in field units (K in mD, β in 1/ft):

1. Geertsma relation [39]:

$$\beta = \frac{48,511.34}{(KK_{rp})^{0.5} (\phi S_p)^{5.5}} \quad (5)$$

2. Frederick and Graves' first relation [40]:

$$\beta = \frac{2.11 \times 10^{10}}{(KK_{rp})^{1.55} (\phi S_p)^{1.0}} \quad (6)$$

3. Frederick and Graves' second relation [40]:

$$\beta = \frac{7.89 \times 10^{10}}{(KK_{rp})^{1.6} (\phi S_p)^{0.404}} \quad (7)$$

The above three relations can be applicable to the single gas phase system and Frederick and Graves' first relation is used to describe the degree of non-Darcy effect in this paper. In order to characterize gas flow accurately, the stress sensitivity is also taken into account in the model. The stress sensitivity of the permeability and porosity can be expressed as:

$$K = K_0 e^{-\alpha(P_{ref}-P)} \tag{8}$$

$$\phi = \phi_a \cdot [1 + C_p(P_{ref} - P)] \tag{9}$$

Substituting Equations (7), (8) and (9) into Equation (1), the flow law equation in field units can be rewritten as:

$$\frac{\rho_g}{\mu_g} e^{-\alpha(P_{ref}-P)} \frac{\partial P}{\partial r} = 11.5741 \frac{\rho_g |v_g|}{K_0} + 1.3396 \times 10^{-13} \frac{\beta \rho_g^2 |v_g|^2}{\mu_g} e^{-\alpha(P_{ref}-P)} \tag{10}$$

The gas velocity can be expressed as:

$$v_g = \frac{Q_g}{2\pi r h} \tag{11}$$

Based on the material balance, the mass flow rate M_r towards the well is given by:

$$M_r = \rho_g Q_g = \rho_{gsc} Q_{gsc} \tag{12}$$

Substituting Equations (11) and (12) into Equation (10), Equation (10) in field units can be rewritten as:

$$\frac{\rho_g}{\mu_g} e^{-\alpha(P_{ref}-P)} \frac{\partial P}{\partial r} = 1.8421 \frac{\rho_{gsc}}{K_0 r h} Q_{gsc} + 1.1133 \times 10^{-14} \frac{\beta \rho_{gsc}^2}{\mu_g r^2 h^2} e^{-\alpha(P_{ref}-P)} Q_{gsc}^2 \tag{13}$$

According to the national standard SY/T 5440-2009 in China, the variation of a steady-state gas well bottom hole pressure should not exceed 0.5% of the current steady flow pressure in the next 8 h. The pressure of a steady-state well is only related to the spatial location, and Equation (13) can be expressed as:

$$\frac{\rho_g}{\mu_g} e^{-\alpha(P_{ref}-P)} \frac{dP}{dr} = 1.8421 \frac{\rho_{gsc}}{K_0 r h} Q_{gsc} + 1.1133 \times 10^{-14} \frac{\beta \rho_{gsc}^2}{\mu_g r^2 h^2} e^{-\alpha(P_{ref}-P)} Q_{gsc}^2 \tag{14}$$

To solve Equation (14), separation of variables method is used to process the gradient term. Integrating Equation (14) over the radius of the well control zone yields Equation (15):

$$\int_{P_{wf}}^{P_e} \frac{\rho_g}{\mu_g} e^{-\alpha(P_{ref}-P)} dP = \int_{r_w}^{r_e} \left(1.8421 \frac{\rho_{gsc}}{K_0 r h} Q_{gsc} + 1.1133 \times 10^{-14} \frac{\beta \rho_{gsc}^2}{\mu_g r^2 h^2} e^{-\alpha(P_{ref}-P)} Q_{gsc}^2 \right) dr \tag{15}$$

The simplified mathematical model is expressed as follows:

$$\int_{P_{wf}}^{P_e} \frac{\rho_g}{\mu_g} e^{-\alpha(P_{ref}-P)} dP = 1.8421 \frac{\rho_{gsc}}{K_0 h} Q_{gsc} \ln\left(\frac{r_e}{r_w}\right) + 1.1133 \times 10^{-14} \frac{\rho_{gsc}^2}{h^2} Q_{gsc}^2 \int_{r_w}^{r_e} \left(\frac{\beta}{\mu_g r^2} e^{-\alpha(P_{ref}-P)} \right) dr \tag{16}$$

If the skin effect is considered, Equation (16) can be changed as follows:

$$\int_{P_{wf}}^{P_e} \frac{\rho_g}{\mu_g} e^{-\alpha(P_{ref}-P)} dP = 1.8421 \frac{\rho_{gsc}}{K_0 h} \ln\left(\frac{r_e}{r_{wr}}\right) Q_{gsc} + 1.1133 \times 10^{-14} \frac{\rho_{gsc}^2}{h^2} Q_{gsc}^2 \int_{r_{wr}}^{r_e} \left(\frac{\beta}{\mu_g r^2} e^{-\alpha(P_{ref}-P)} \right) dr \tag{17}$$

where $r_{wr} = r_w e^{-S}$, and S is the skin factor.

Defining the function of gas-phase pseudo-pressure:

$$\varphi(P) = \int_{P_m}^P \frac{\rho_g}{\mu_g} e^{-\alpha(P_{ref}-P)} dP \tag{18}$$

The simplified mathematical model is expressed as follows:

$$\Delta\varphi = A Q_{gsc} + B(P) Q_{gsc}^2 \tag{19}$$

where:

$$\begin{cases} \Delta\varphi = \varphi(P_e) - \varphi(P_{wf}) \\ A = 1.8421 \frac{\rho_{gsc}}{K_0 h} \ln\left(\frac{r_e}{r_w}\right) \\ B(P) = 1.1133 \times 10^{-14} \frac{\rho_{gsc}^2}{h^2} \int_{r_w}^{r_e} \left(\frac{\beta}{\mu_g r^2} e^{-\alpha(P_{ref}-P)}\right) dr \end{cases} \tag{20}$$

Once the flow parameters are obtained, the surface gas flow rate, Q_{gsc} , at any other flow pressure is obtained from Equation (19):

$$Q_{gsc} = \frac{-A + \sqrt{A^2 + 4B \cdot \Delta\varphi}}{2B(P)} \tag{21}$$

Thus, the mathematical model to estimate the inflow performance relationship is established.

3. Solving Method of the Mathematical Model

Coefficient B in Equation (19) is variable with pressure, so it is necessary to describe the pressure profile in the entire gas reservoir. In order to get the distribution of pressure along the radial direction, the radial length is logarithmically divided into N segments, as shown in Figure 3.

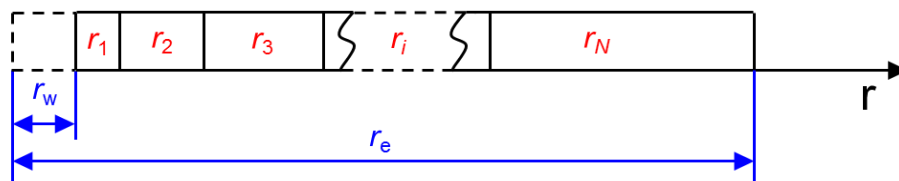


Figure 3. Schematic diagram of grid discretization.

Suppose the discrete reference block in space is the i th block, and the discrete reference point in time is the $(n + 1)$ th time step. For the i th block, the equation is shown as follows:

$$A_2 P_{i-1}^{n+1} - (A_1 + A_2 + B_1) P_i^{n+1} + A_1 P_{i+1}^{n+1} = -B_1 P_i^n \tag{22}$$

where

$$\begin{cases} A_1 = \frac{r_{i+\frac{1}{2}} \left(\rho \delta \frac{K}{\mu}\right)_{i+\frac{1}{2}}^{n+1}}{r_i \cdot \Delta r_{i+\frac{1}{2}} \cdot \left(r_{i+\frac{1}{2}} - r_{i-\frac{1}{2}}\right)} \\ A_2 = \frac{r_{i-\frac{1}{2}} \left(\rho \delta \frac{K}{\mu}\right)_{i-\frac{1}{2}}^{n+1}}{r_i \cdot \Delta r_{i-\frac{1}{2}} \cdot \left(r_{i+\frac{1}{2}} - r_{i-\frac{1}{2}}\right)} \\ B_1 = \frac{\left(\frac{\partial \rho}{\partial P} \phi + \phi_0 C_p \rho\right)_i^n}{t^{n+1} - t^n} \end{cases} \tag{23}$$

As the physical quantity $\left(\rho \delta \frac{K}{\mu}\right)$ in Equation (23) is a function of space and time, the upwind scheme is used to assign values to physical quantities on the grid points. The upwind scheme is shown as follows:

$$\left(\rho \delta \frac{K}{\mu}\right)_{i+\frac{1}{2}}^{n+1} = \begin{cases} \left(\rho \delta \frac{K}{\mu}\right)_i^n & \text{If the fluid goes from } i \text{ to } i+1 \\ \left(\rho \delta \frac{K}{\mu}\right)_{i+1}^n & \text{If the fluid goes from } i+1 \text{ to } i \end{cases} \tag{24}$$

After the upwind scheme processing, Equation (23) can be rewritten as:

$$\begin{cases} A_1 = \frac{r_{i+\frac{1}{2}} \left(\rho \delta \frac{K}{\mu} \right)_{i+1}^n}{r_i \cdot \Delta r_{i+\frac{1}{2}} \cdot \left(r_{i+\frac{1}{2}} - r_{i-\frac{1}{2}} \right)} \\ A_2 = \frac{r_{i-\frac{1}{2}} \left(\rho \delta \frac{K}{\mu} \right)_i^n}{r_i \cdot \Delta r_{i-\frac{1}{2}} \cdot \left(r_{i+\frac{1}{2}} - r_{i-\frac{1}{2}} \right)} \\ B_1 = \frac{\left(\frac{\partial \rho}{\partial P} \phi + \phi_0 C_p \rho \right)}{t^{n+1} - t^n} \end{cases} \quad (25)$$

Then, the pressure distribution can be calculated from the well bottom to the reservoir boundary by using Gaussian elimination with scaled partial pivoting. The detailed solution process of the model is shown as a flowchart in Figure 4.

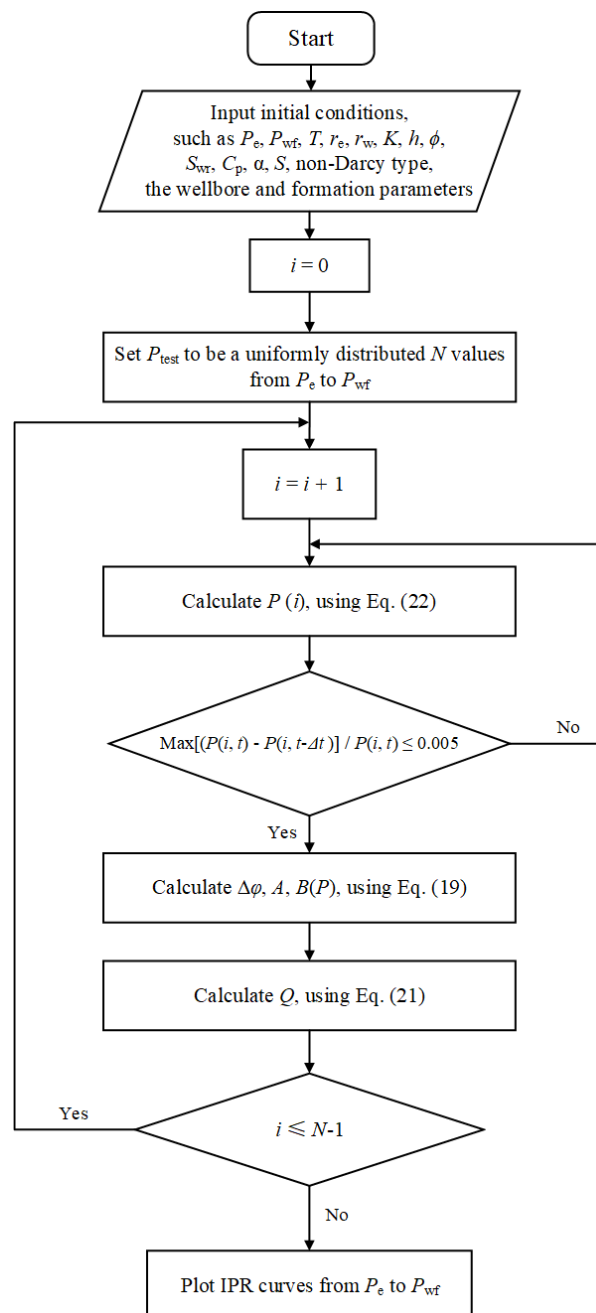


Figure 4. Calculation flow chart for gas reservoir pressure distribution.

4. Results and Discussion

4.1. Model Validation

To validate this new model, the calculation results of this model are compared with simulated results, as shown in Figure 5. The key parameters obtained from the geological model for model validation are listed in Table 1.

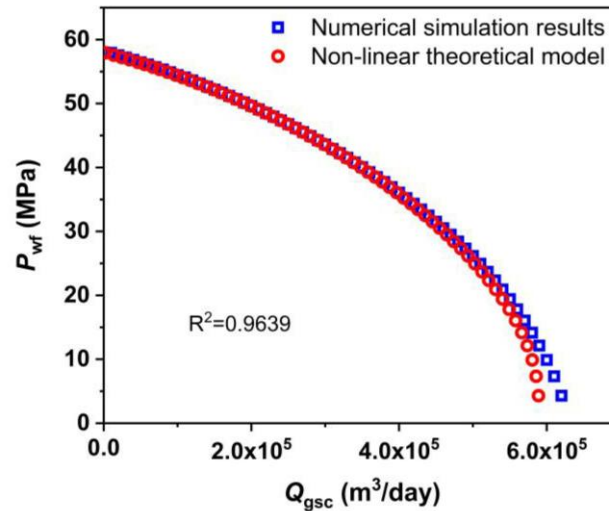


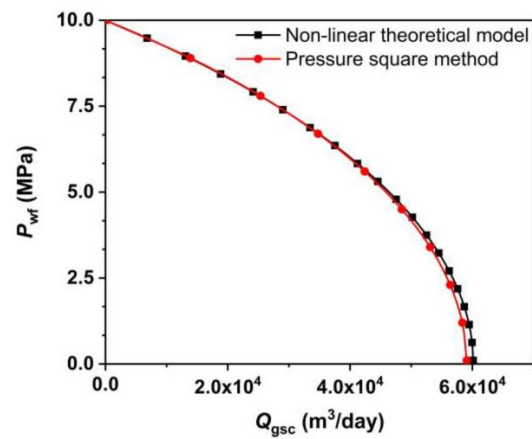
Figure 5. Comparison of the calculation results and simulated results.

Table 1. The key parameters obtained from the geological model for model validation.

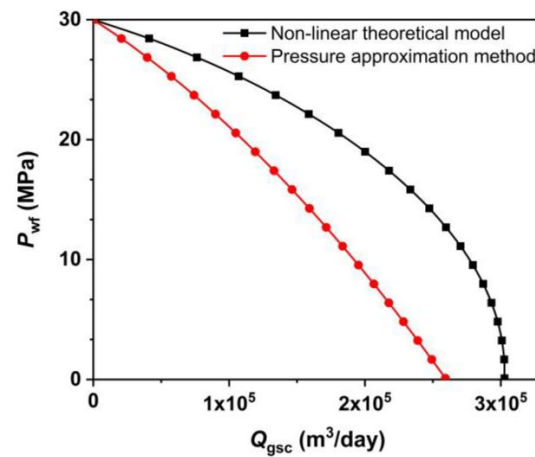
Parameters	Value	Unit
Reservoir thickness	45	m
Porosity	0.07	-
Permeability	1	mD
Original reservoir pressure	58	MPa
Reservoir temperature	116	°C
Initial gas saturation	0.4	-
Drainage radius	500	m
Wellbore radius	0.0762	m

Figure 5 shows that the simulated results and the calculation results of this model have a very good match. Therefore, this model can provide a reasonable prediction of gas production rate in the reservoir.

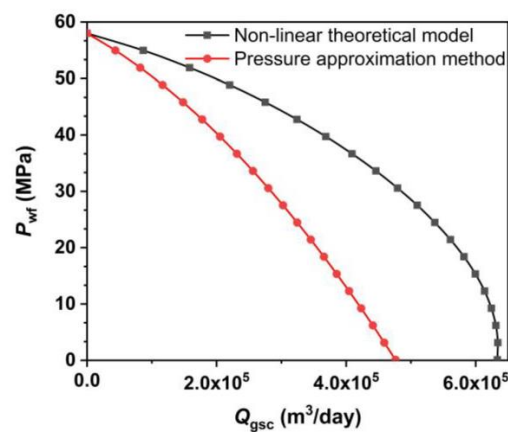
Then, a comparative study of the non-linear theoretical model results and the linearization method results was conducted at three different pressure conditions (Figure 6). Figure 6a shows that the results of pressure square method at low pressure have a good match with the predicted results of this model. This linearization method is acceptable for use in the prediction of inflow performance. Figure 6b shows that the deviation between the non-linear theoretical model and the pressure approximation method became greater within the pressure of 25–30 MPa. When the test pressure was high, the error of 22.58% indicates that the linearization method is not reliable for dealing with nonlinear equations, as shown in Figure 6c.



(a)



(b)



(c)

Figure 6. Comparison of the predicted results with linearization methods at three different pressure conditions: (a) IPR curves made by non-linear theoretical model and pressure square method within the well bottom hole pressure of 0.1–10 MPa, (b) IPR curves made by non-linear theoretical model and pressure approximation method within the well bottom hole pressure of 0.1–30 MPa (c) IPR curves made by non-linear theoretical model and pressure approximation method within the well bottom hole pressure of 0.1–58 MPa.

4.2. Effect of Reservoir Permeability

The effect of permeability on gas production was analyzed, as shown in Figure 7. Figure 7a shows the inflow performance relationship curves at different reservoir permeabilities. It can be seen that the higher reservoir permeability greatly increased the absolute open flow rate. With the increase of gas reservoir permeability, the slope of the curves gradually decreases, indicating that the unit production pressure difference corresponds to a higher productivity. In ultra-low-permeability reservoirs ($K < 0.1$ mD), a high production pressure difference will not help the production. Further analysis of the bottom hole flow characteristics was conducted. In Figure 7b, the straight pink line represents the relationship between well bottom hole pressure and flow rate in the Darcy flow condition and the black curve indicates that flow has non-Darcy characteristics. The gas flow is mainly controlled by viscous force (v term) and inertial force (v^2 term). Figure 7b shows that due to the increased permeability, the proportion of flow controlled by viscous force continues to decrease, from 9.34% to 2.96%. At the same time, inertial force is always in the dominant position, controlling 90% of the flow. The high flow rate enhances the influence of inertial resistance. For the high-velocity flow, the v^2 quadratic term tends to the limit, so a third term of the velocity form is necessary to describe the high-velocity non-Darcy effect.

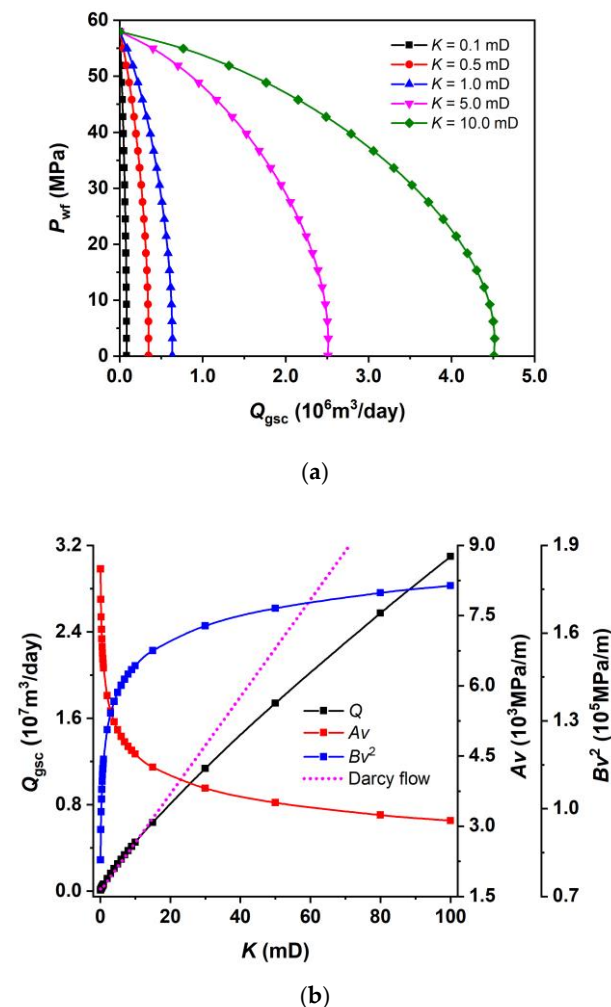


Figure 7. Effect of reservoir permeability on gas production rate and flow characteristics. (a) IPR curves with different permeabilities. (b) Characteristic analysis of flow regime at the well bottom hole.

4.3. Effect of Original Reservoir Pressure

Since the gas isothermal coefficient of compressibility is greater than the rock compressibility, the original reservoir pressure determines the elastic energy of the gas reservoir. The effect of original reservoir pressure on the gas inflow performance relationship was analyzed, and the results are presented in Figure 8.

Figure 8a shows that for the same bottom hole pressure, wells drilled in reservoirs with the higher original reservoir pressure have the higher production rate. From Equation (1), one would expect that a high original reservoir pressure is equivalent to a high gas pseudo-pressure. For the same flow resistance, this means high productivity.

Figure 8b shows that a high original reservoir pressure increases the gas production rate, and enhances the flow controlled by viscous force and inertial force to different degrees. With the increase of the original reservoir pressure, the pressure losses caused by both viscous force and inertial force increase at the well bottom. The portion of the viscous flow influenced by the high production rate decreases from 16.33% to 5.01%. Because of the high velocity at the well bottom, the inertial force is still dominant.

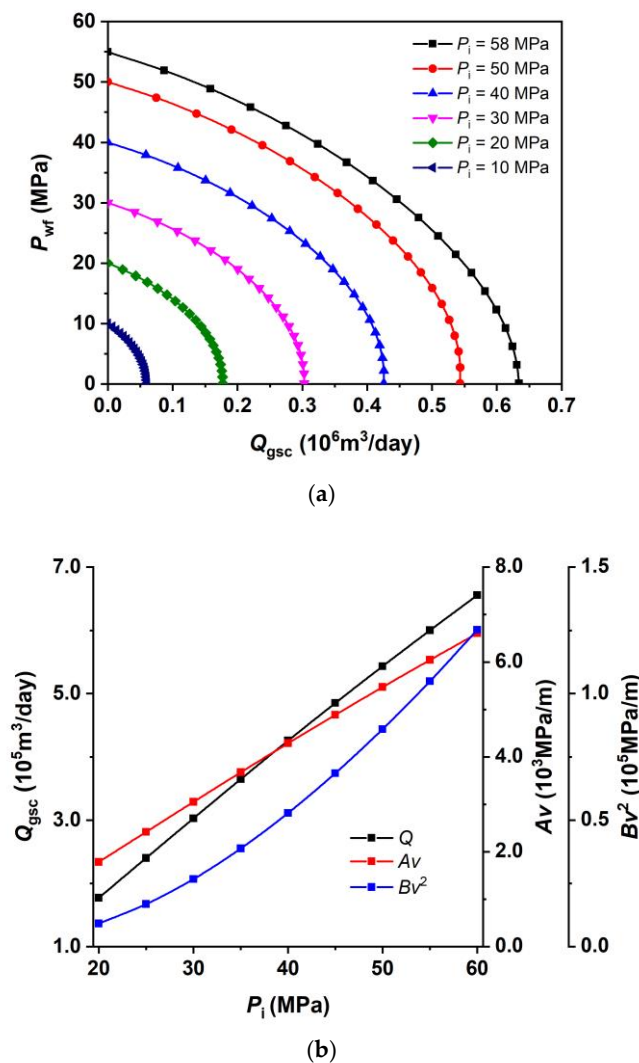


Figure 8. Effect of original reservoir pressure on gas production rate and flow characteristics. (a) IPR curves with different original reservoir pressure. (b) Characteristic analysis of flow regime at the well bottom.

4.4. Effect of Initial Gas Saturation

In the whole seepage process, the porosity directly determines the reserves. The effect of initial gas saturation on the gas inflow performance relationship was analyzed, and the results are presented in Figure 9. From Equation (7), the porosity has a slight influence on the β coefficient and the inertial force, and will eventually have an impact on the absolute open flow rate (Figure 9a). Figure 9b shows that with the increase of pressure loss caused by the viscous force, the pressure loss caused by inertial force decreases from 94.82% to 94.26%. The high-velocity non-Darcy effect cannot be ignored. The inertial force is dominant.

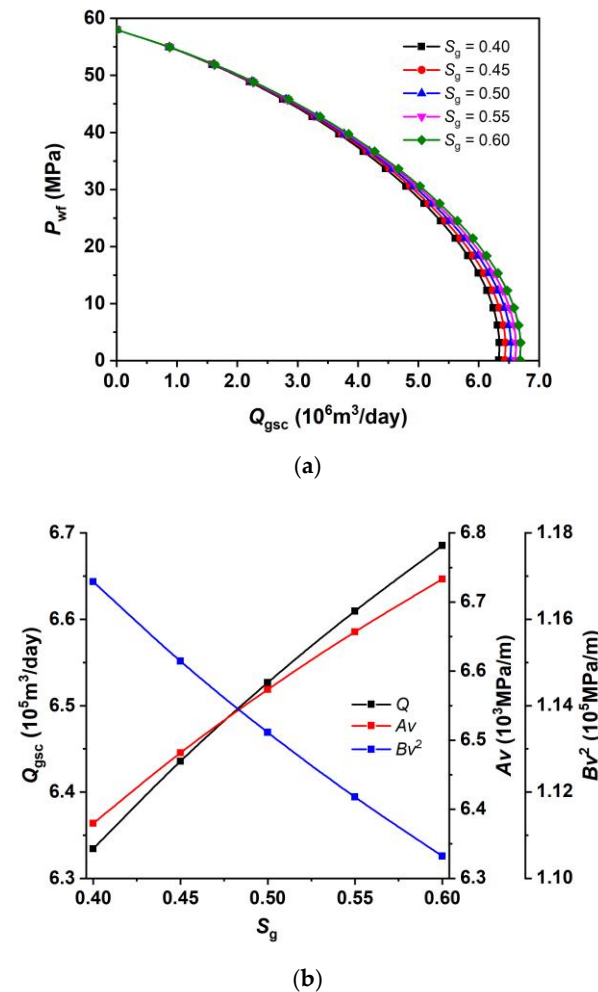


Figure 9. Effect of initial gas saturation on gas production rate and flow characteristics. (a) IPR curves with different initial gas saturation. (b) Characteristic analysis of flow regime at the well bottom hole.

4.5. Effect of Stress Sensitivity Coefficient

The reservoir permeability is the key parameter affecting the inflow performance relationship, as shown in Figure 10. Figure 10a shows that a higher stress sensitivity coefficient results in a lower absolute open flow rate and a faster decreasing trend of production rate. As the stress sensitivity coefficient increases, the stress sensitivity of the reservoir increases. This shows that under the same bottom hole pressure condition, the permeability of the near-wellbore will drop sharply. In Figure 10b, with the increase of stress sensitivity coefficient, gas velocity decreases, and pressure losses caused by viscous force and inertial force increase. The rate of seepage resistance increased by the drop in permeability is much greater than the rate of pressure gradient change. More than 94.82% of the pressure gradient is consumed by inertial force, and the inertial force is still dominant.

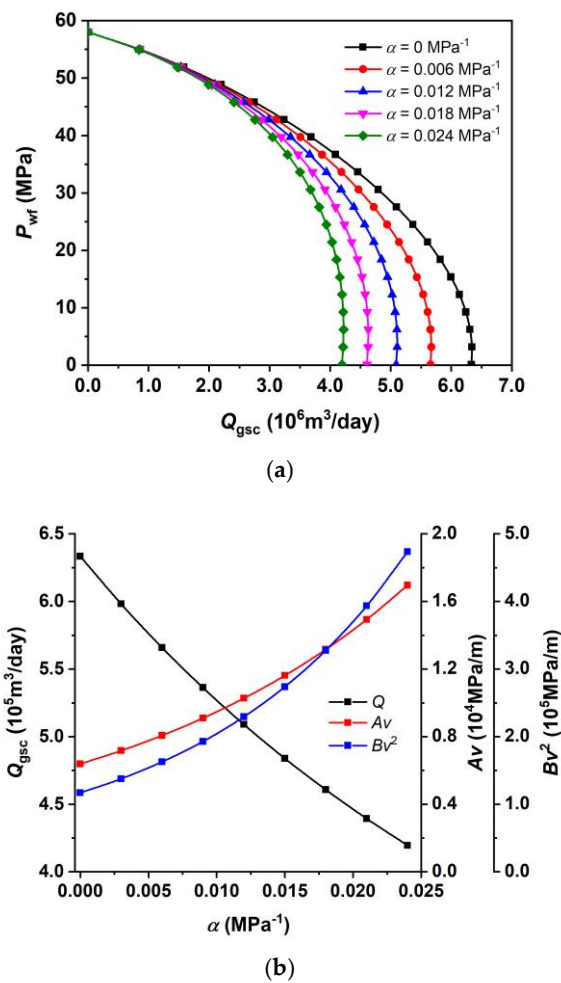


Figure 10. Effect of stress sensitivity coefficient on gas production rate and flow characteristics. (a) IPR curves with different stress sensitivity coefficient. (b) Characteristic analysis of flow regime at the well bottom hole.

4.6. Effect of Skin Factor

For the wells with imperfect hydrodynamics, the radius of an imperfect well can be replaced with that of a hypothetical perfect well. The effect of skin factor on the gas inflow performance relationship was analyzed, and the results are presented in Figure 11. Figure 11a shows that a lower skin factor results in a higher production rate. Even though a field has a high permeability, the productivity of a well with a high skin factor cannot be increased without taking measures. In Figure 11b, with the increase of skin factor, absolute open flow rate decreases, and gas velocity and pressure losses caused by viscous force and inertial force increase. The converted radius of the imperfect well has a great influence on the gas flow velocity. Therefore, the minimum value of flow velocity at the bottom hole corresponds to the maximum value of the absolute flow rate. When the skin coefficient is equal to 3, the gas velocity is the greatest, and the proportion of pressure caused by inertial force can reach 99.07%. In the case of a skin coefficient equal to -3 , the gas velocity is the lowest, and the proportion of pressure caused by inertial force can reach 70.64%. The inertial force is still dominant.

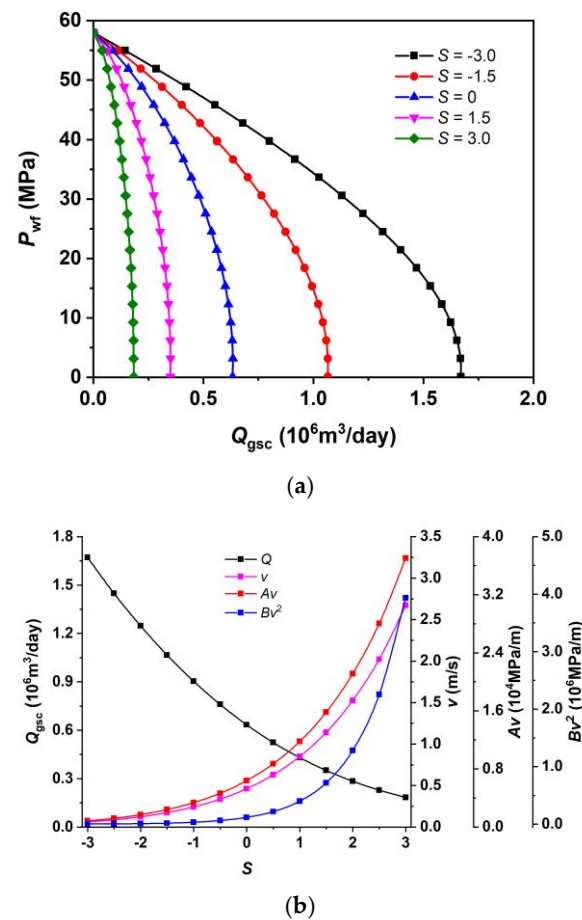


Figure 11. Effect of skin factor on gas production rate and flow characteristics. (a) IPR curves with different skin factors. (b) Characteristic analysis of flow regime at the well bottom hole.

5. Field Application

The Bereketli-Pirgui gas field is located on the right bank of the Amu Darya River. The gas-bearing area is 21.72 km^2 and the geological reserves is $201.97 \times 10^8 \text{ m}^3$. The reservoir depth is 3127.63 m . The initial reservoir temperature is $112.619 \text{ }^\circ\text{C}$, and the pressure is 53.47 MPa . As of August 2020, there were 22 gas wells in the block, and most of the production wells only produce gas. The inflow performance relationship of the gas wells is unclear, and the production system has not been determined. Therefore, it is significant to develop a model to evaluate the IPR with high precision and establish a rational proration plan.

The target layer was layer XVa1, and the average permeability of this layer was 1.03 mD . In March 2019, a well test was carried out on well Pir-21. The Pir-21 well test data are shown in Table 2. A production pressure difference of less than 3 MPa is suitable for a well test. Firstly, a small production pressure difference ensures that the well bottom hole pressure will become stable quickly. Second, a small production pressure difference guarantees that the reservoir fluid properties that are strongly dependent on pressure are not changed drastically.

Table 2. Pir-21 well test data.

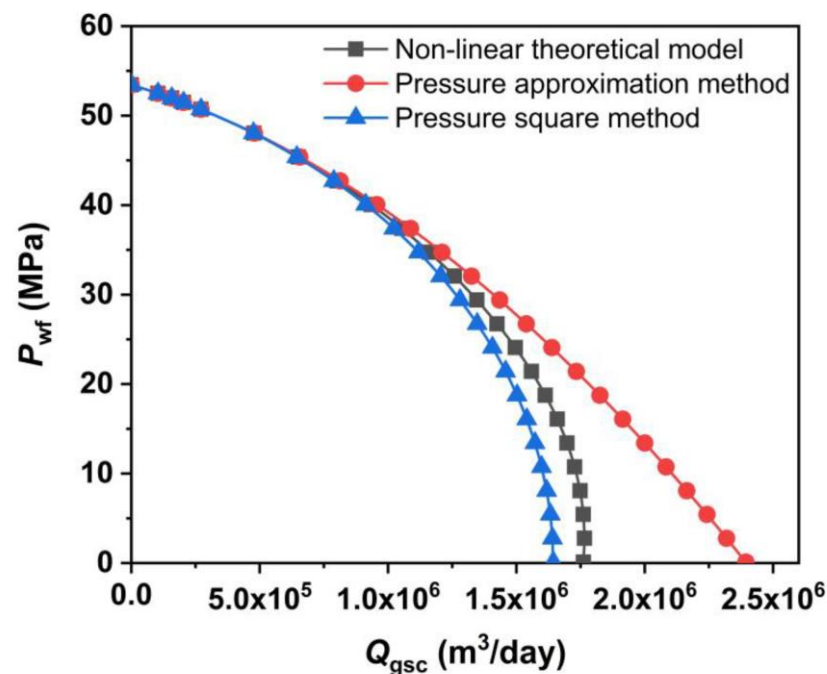
Test Date	Test Phase	Test Time (h)	Daily Surface Gas Production Rate ($10^4 \text{ m}^3/\text{d}$)	Well Bottom Hole Pressure (MPa)
2019.3.13–3.25	Productivity test	8	10.34	52.5
		8	15.75	51.96
		8	20.29	51.48
		8	27.14	50.71
	Well shut-in	30		53.44

In this context, coefficients A and B of Equation (19) can be treated as constant. For linear regression, Equation (19) can be expressed as:

$$\frac{\Delta\varphi}{Q_{gsc}} = A + BQ_{gsc} \quad (26)$$

The values of A and B can be obtained by the fitting relationship between Q_{gsc} and $\Delta\varphi/Q_{gsc}$ as shown in Equation (26), and their values are 6.6608×10^{-5} and 4.4411×10^{-11} , respectively.

According to Equation (20), the flowability coefficient K_0h can be calculated, and is equal to 165.2030 mD·m. Based on the well logging test, the value of reservoir effective thickness is 68.78 m. Accordingly, the effective horizontal permeability is 2.4019 mD. The results are satisfying and indicate that this model is an effective approach to obtain reservoir parameters in gas reservoirs. Based on the Pir-21 well test data, the model presented in this paper and traditional linearization methods (e.g., pressure square method and pressure approximation method) were used to predict the inflow performance relationship, as shown in Figure 12.

**Figure 12.** Inflow performance relationship of different methods.

The results of traditional linearization methods greatly underestimate the productivity of the gas wells, with an error up to 35.93%. It is noticeable that the model in this paper can fully consider the impact of the stress sensitivity, the gas high-velocity non-Darcy effect, and the change of gas properties on gas well productivity.

6. Conclusions

In this study, a novel mathematical model considering real gas PVT behavior was developed. The pseudo-pressure function and gas properties database are introduced to improve the accuracy of this model which estimates the inflow performance relationship of gas well production. On this basis, the effects of reservoir permeability, original reservoir pressure, initial gas saturation, stress sensitivity coefficient, and skin factor on the inflow performance relationship of gas reservoir production were analyzed by this model. Based on the results, several conclusions are obtained as follows:

1. A novel mathematical model considering real gas PVT behavior is developed to accurately estimate the inflow performance relationship of gas well production.
2. For gas flow equations, the errors caused by traditional linearization methods and empirical formulas lead to the underestimation of gas well productivity.
3. The results show that more than 90% of the energy in the flow field is consumed by inertial forces, which leads to significant high-velocity non-Darcy effects in the gas reservoir.
4. The reservoir permeability, original reservoir pressure, stress sensitivity coefficient, and skin factor have a great impact on the IPR of gas reservoir production.
5. This model predicts gas IPR curves with excellent accuracy and high efficiency. The high-precision gas well inflow performance relationship lays a solid foundation for dynamic production analysis, rational proration, and intelligent development of gas fields.

Author Contributions: Investigation, S.Z.; Methodology S.Z.; Resources Y.G.; Data curation K.S.; Supervision H.L.; Validation Y.W.; Writing—original draft, S.Z. Writing—review and editing, S.Z. All authors have read and agreed to the published version of the manuscript.

Funding: This research was funded by Joint Fund for Enterprise Innovation and Development of National Natural Science Foundation of China, grant number U19B6003-02-06 and National Natural Science Foundation of China, grant number 51974331.

Institutional Review Board Statement: Not applicable.

Informed Consent Statement: Not applicable.

Data Availability Statement: Not applicable.

Acknowledgments: This work was supported by the Joint Fund for Enterprise Innovation and Development of the National Natural Science Foundation of China (Grant No. U19B6003-02-06) and the National Natural Science Foundation of China (Grant No. 51974331). The authors would like to sincerely acknowledge these funds for their financial support. Finally, Shuang Z. wants to thank, in particular, the unreserved support received from Zhiqing C. in these years. Will you marry me?

Conflicts of Interest: The authors declare no conflict of interest.

Nomenclature

a	Viscosity flow coefficient, Pa·s/m ²
A	First-order coefficient of gas surface flow, 10 ¹⁸ kg/m ⁶
A_1, A_2	Coefficients of the coefficient matrix, dimensionless
b	Inertial flow coefficient, Pa·s ² /m ³
B	First-order coefficient of gas surface flow, 10 ¹⁸ kg·day/m ⁹
B_1	Coefficient of constant term, dimensionless
C_p	Compressibility of pore space of rock, MPa ⁻¹
h	Reservoir thickness, m
K	Effective reservoir permeability, mD
K_o	Original reservoir permeability, mD
K_{rp}	Relative permeability of phase, dimensionless
K_{0-h}	Flowability coefficient, mD·m
P	Pressure, MPa

P_e	Original pressure, MPa
P_{ref}	Reference pressure, MPa
P_{wf}	Bottom hole pressure, MPa
Q_g	Gas flow rate at reservoir condition, m ³ /day
Q_{gsc}	Gas flow rate at surface condition, m ³ /day
r	Radial distance, m
r_e	Supply boundary radius, m
r_w	Well radius, m
S	Skin factor, dimensionless
S_p	Saturation of phase, dimensionless
Greek	
α	Stress sensitivity coefficient, MPa ⁻¹
β	Forchheimer factor, m ⁻¹
ϕ	Porosity, dimensionless
μ_g	Gas viscosity, mPa·s
v_g	Gas velocity, m/day
ρ_g	Gas density in reservoir condition, g/cm ³
ρ_{gsc}	Gas density in standard condition, g/cm ³
Subscript	
g	Gas phase
gsc	Gas in standard condition

References

- Muskat, M. The Flow of Homogeneous Fluids Through Porous Media. *J. Geol.* **1938**, *46*, 6. [[CrossRef](#)]
- Evinger, H.H.; Muskat, M. Calculation of Theoretical Productivity Factor. *Trans. AIME* **1942**, *146*, 126–139. [[CrossRef](#)]
- Gilbert, W.E. Flowing and gas-lift well performance. In Proceedings of the Drilling and Production Practice, Los Angeles, CA, USA, 1 January 1954.
- Weller, W.T. Reservoir Performance During Two-Phase Flow. *J. Pet. Technol.* **1966**, *18*, 240–246. [[CrossRef](#)]
- Vogel, J. Inflow Performance Relationships for Solution-Gas Drive Wells. *J. Pet. Technol.* **1968**, *20*, 83–92. [[CrossRef](#)]
- Standing, M.B. Inflow Performance Relationships for Damaged Wells Producing by Solution-Gas Drive. *J. Pet. Technol.* **1970**, *22*, 1399–1400. [[CrossRef](#)]
- Fetkovich, M.J. The isochronal testing of oil wells. In Proceedings of the Fall Meeting of the Society of Petroleum Engineers of AIME, Dallas, TX, USA, 30 September–3 October 1973.
- Klins, M.A.; Majcher, M.W. Inflow Performance Relationships for Damaged or Improved Wells Producing Under Solution-Gas Drive. *J. Pet. Technol.* **1992**, *44*, 1357–1363. [[CrossRef](#)]
- Sajedian, A.; Ebrahimi, M.; Jamialahmadi, M. Two-phase inflow performance relationship prediction using two artificial intelligence techniques: Multi-layer perceptron versus genetic programming. *Pet. Sci. Technol.* **2012**, *30*, 1725–1736. [[CrossRef](#)]
- Dietz, D.N. Determination of Average Reservoir Pressure from Build-Up Surveys. *J. Pet. Technol.* **1965**, *17*, 955–959. [[CrossRef](#)]
- Economides, M.J.; Deimbacher, F.X.; Brand, C.W.; Heinemann, Z.E. Comprehensive simulation of horizontal well performance. *SPE Form. Eval.* **1997**, *6*, 418–426. [[CrossRef](#)]
- Aronofsky, J.S.; Jenkins, R. A Simplified Analysis of Unsteady Radial Gas Flow. *J. Pet. Technol.* **1954**, *6*, 23–28. [[CrossRef](#)]
- Jones, L.; Blount, E.; Glaze, O. Use of short term multiple rate flow tests to predict performance of wells having turbulence. In Proceedings of the SPE Annual Fall Technical Conference and Exhibition, New Orleans, LA, USA, 3–6 October 1976.
- Odeh, A. Pseudosteady-State Flow Equation and Productivity Index for a Well with Noncircular Drainage Area. *J. Pet. Technol.* **1978**, *30*, 1630–1632. [[CrossRef](#)]
- Tian, L.; Shen, Y.H.; Wang, S.J.; He, S.L. A new real-time gas well productivity evaluating method. *Adv. Mater. Res.* **2011**, *433*, 1078–1084. [[CrossRef](#)]
- Massmann, J.W. Applying Groundwater Flow Models in Vapor Extraction System Design. *J. Environ. Eng.* **1989**, *115*, 129–149. [[CrossRef](#)]
- Baehr, A.L.; Hult, M.F. Evaluation of Unsaturated Zone Air Permeability Through Pneumatic Tests. *Water Resour. Res.* **1991**, *27*, 2605–2617. [[CrossRef](#)]
- Guo, W.X. Analytical solution of transient radial air flow to an extraction well. *J. Hydrol.* **1997**, *194*, 1–14. [[CrossRef](#)]
- Di Giulio, D.C.; Varadhan, R. Development of Recommendations and Methods to Support Assessment of Soil Venting Performance and Closure. Ph.D. Thesis, The University of Arizona, Phoenix, AZ, USA, 2000.
- Raghavan, R. Well Test Analysis: Wells Producing by Solution Gas Drive. *Soc. Pet. Eng. J.* **1976**, *16*, 196–208. [[CrossRef](#)]
- Fevang, O. Gas Condensate Flow Behavior and Sampling. Ph.D. Thesis, Norges Tekniske Hogskole, Trondheim, Norway, 1995.

22. Wang, Y.; Liu, H.; Zhou, Y. Development of a deep learning-based model for the entire production process of steam-assisted gravity drainage (SAGD). *Fuel* **2021**, *287*, 119565. [[CrossRef](#)]
23. Wang, Y.; Liu, H.; Wang, J.; Dong, X.; Chen, F. Formulation development and visualized investigation of temperature-resistant and salt-tolerant surfactant-polymer flooding to enhance oil recovery. *J. Pet. Sci. Eng.* **2019**, *174*, 584–598. [[CrossRef](#)]
24. Al-Hussainy, R.; Ramey, H.J.; Crawford, P.B. The Flow of Real Gases Through Porous Media. *J. Pet. Technol.* **1966**, *18*, 624–636. [[CrossRef](#)]
25. Raghavan, R.; Scorer, J.D.T.; Miller, F.G. An Investigation by Numerical Methods of the Effect of Pressure-Dependent Rock and Fluid Properties on Well Flow Tests. *Soc. Pet. Eng. J.* **1972**, *12*, 267–275. [[CrossRef](#)]
26. Samaniego, V.F.; Brigham, W.E.; Miller, F.G. An investigation of transient flow of reservoir fluids considering pressure-dependent rock and fluids properties. *SPE J.* **1977**, *17*, 141–150. [[CrossRef](#)]
27. Samaniego, V.F.; Brigham, W.E.; Miller, F.G. Performance-prediction procedure for transient flow of fluids through pressure-sensitive formations. *J. Petrol. Technol.* **1979**, *31*, 779–786. [[CrossRef](#)]
28. Dranchuk, P.M.; Abou-Kassem, J.H. Calculation of Z Factors for Natural Gases Using Equations of State. *J. Can. Pet. Technol.* **1975**, *14*, 34–36. [[CrossRef](#)]
29. Lee, A.L.; Gonzalez, M.H.; Eakin, B.E. The Viscosity of Natural Gases. *J. Pet. Technol.* **1966**, *18*, 997–1000. [[CrossRef](#)]
30. Setzmann, U.; Wagner, W. A New Equation of State and Tables of Thermodynamic Properties for Methane Covering the Range from the Melting Line to 625 K at Pressures up to 100 MPa. *J. Phys. Chem. Ref. Data* **1991**, *20*, 1061–1155. [[CrossRef](#)]
31. Mulero, A.; Cachadi, A.I. Recommended correlations for the surface tension of several fluids included in the REFPROP program. *J. Phys. Chem. Ref. Data* **2014**, *43*, 169. [[CrossRef](#)]
32. Forchheimer, P.H. Wasserbewegung durch boden. *VDI Z.* **1901**, *45*, 1782–1788.
33. Smith, V. Unsteady-state gas flow into gas wells. *J. Petrol. Technol.* **1961**, *13*, 1151–1159. [[CrossRef](#)]
34. Swift, G.W.; Kiel, O.G. The Prediction of Gas-Well Performance Including the Effect of Non-Darcy Flow. *J. Pet. Technol.* **1962**, *14*, 791–798. [[CrossRef](#)]
35. Yang, J.; He, F.; Zou, Y. A study on dynamic productivity calculation for gas well using data from pressure transient testing. *Nat. Gas Ind.* **2007**, *27*, 95–96.
36. Li, X.; Hu, Y. A discussion on the transient inflow performance relationship curve of gas-water well. *Nat. Gas Ind.* **2001**, *21*, 65–67.
37. Zhang, L.; Zhu, S.; Wang, K.; Zhou, L. Study of the high speed non-Darcy gas percolation model. *Xinjiang Pet. Geol.* **2004**, *25*, 165–167.
38. Clarkson, C.R.; Qanbari, F.; Nobakht, M.; Heffner, L. Incorporating Geomechanical and Dynamic Hydraulic-Fracture-Property Changes into Rate-Transient Analysis: Example from the Haynesville Shale. *SPE Reserv. Eval. Eng.* **2013**, *16*, 303–316. [[CrossRef](#)]
39. Geertsma, J. Estimating the Coefficient of Inertial Resistance in Fluid Flow Through Porous Media. *Soc. Pet. Eng. J.* **1974**, *14*, 445–450. [[CrossRef](#)]
40. Frederick, D.; Graves, R. New correlations to predict non-Darcy flow coefficients at immobile and mobile water saturation. In Proceedings of the SPE Annual Technical Conference and Exhibition, New Orleans, LA, USA, 28 September 1994.